

# Analog 28 GHz LoS MIMO Relay System Using a 90° Hybrid Coupler

Joerg Eisenbeis\*, *Student Member, IEEE*, Yueheng Li, *Student Member, IEEE*, Jerzy Kowalewski, *Member, IEEE*, Marius Kretschmann, and Thomas Zwick, *Fellow, IEEE*

**Abstract**—To enlarge the range of wireless fronthaul and backhaul communication links operating close to the millimeter-wave (mmW) region, this work presents a novel Line-of-Sight (LoS) Multiple-Input Multiple-Output (MIMO) relay system. The analog relay system consists of a simple 90° hybrid coupler to separate two uncorrelated transmit data streams realizing a low-complex and cheap system. The functional capability is proven within measurements of two independent  $2 \times 2$  LoS MIMO links at 28 GHz connected by the relay system. A high decoupling of the two independent transmitted data streams of more than 27 dB after the 90° hybrid coupler and a high modulation error rate (MER) at the last receiver of around 22 dB could be reached for QPSK and 16-QAM modulated signals.

**Index Terms**—MIMO, Relay networks

## I. INTRODUCTION

To overcome the bandwidth shortage in the frequency spectrum below 6 GHz, next-generation mobile communication systems will exploit the mmW spectrum [1]–[3]. One interesting frequency band lately specified by the 3rd generation partnership project is the *n257* band ranging from 26.5 GHz to 29.5 GHz [4]. Within this frequency band directional high data rate links are required for mobile radio communication networks for fronthaul and backhaul communication [5]. These links allow to transport the growing amount of mobile data towards the backbone and enable a flexible connection between mobile radio base stations. To bridge larger distances or blocked LoS connections relay systems are required [6]. To further increase the data rate of directional links so-called LoS MIMO systems can be used [7]–[14]. In general, multiple independent transmitted data streams radiated via parallel wireless communication links would interfere with each other. However, by correct adjustment of the antenna spacing at the transmitter and receiver, the parallel transmitted data streams can be separated by equalization at the receiver [15]. The spatial distance between the multiple transmit and receive antennas thereby depends mainly on the distance between transmitter and receiver [16]. This principle works in contrast to classical spatial multiplexing techniques used in MIMO communication also in purely directional links, i.e. communication links without any multipath channel [15], [17].

This work was supported by the European Union and the German Federal Ministry of Education and Research in frame of the ECSEL Joint Undertaking project TARANTO under grant number 16ESE0211 as well as the German Research Foundation in frame of the METABEAM project under grant number ZW180/22-1.

The authors are with the Institute of Radio Frequency Engineering and Electronics (IHE), Karlsruhe Institute of Technology (KIT), Kaiserstr. 12, 76131 Karlsruhe, Germany. E-mail: \*joerg.eisenbeis@kit.edu.

To reduce the system complexity several LoS MIMO demonstrators have been presented in literature using analog equalization circuitry at the receiver [8], [18]–[22]. In this work we simplify the concept of the analog equalization to its minimum, by employing a single 90° hybrid coupler. This approach drastically reduces the hardware complexity and thereby lowers costs. The high decoupling of the parallel transmitted data streams after the 90° hybrid coupler is verified within measurements. Furthermore, the concept of a transparent communication link through the relay system by connecting two  $2 \times 2$  LoS MIMO links operating at 28 GHz is proven.

## II. LOS MIMO USING ANALOG BEAMFORMING

In wireless propagation scenarios, without any multipath propagation, a spatial multiplexing gain can be achieved by correct adjustment of the transmit and receive antenna spacing [16], [23]. The optimum antenna spacing is given by [11]

$$d_{\text{opt}} = \sqrt{\frac{\lambda \cdot d_c}{N}} \cdot K \quad (1)$$

with  $K = 2i + 1$  and  $i \in \mathbb{N}_0$ , where  $\lambda$  represents the signal wavelength,  $d_c$  the distance between the transmitter and receiver and  $N$  the number of antennas at each side. At the receiver the uncorrelated transmit data streams can be recovered using analog or digital channel equalization. Especially, analog channel equalizers are interesting for relay systems as analog-to-digital and digital-to-analog conversion as well as digital signal processing is not necessary. This drastically reduces the hardware and operation costs.

### A. 90° Hybrid Coupler Concept

By employing a 90° hybrid coupler with its transfer matrix [24]

$$\mathbf{T} = \frac{-1}{\sqrt{2}} \begin{pmatrix} j & 1 \\ 1 & j \end{pmatrix} \quad (2)$$

the over the air superimposed uncorrelated signals, sent from each antenna independently, can be recovered. Important is an adjustment of the received power and an equal group delay from the receive antennas to the corresponding input port of the 90° hybrid coupler, as imbalances in amplitude and phase will cause crosstalk between the two independent data streams. It should be noted, that for large distances  $d_c \gg d_{\text{opt}}$  between the transmitter and receiver the received power will be approximately identical. However, differences in phase

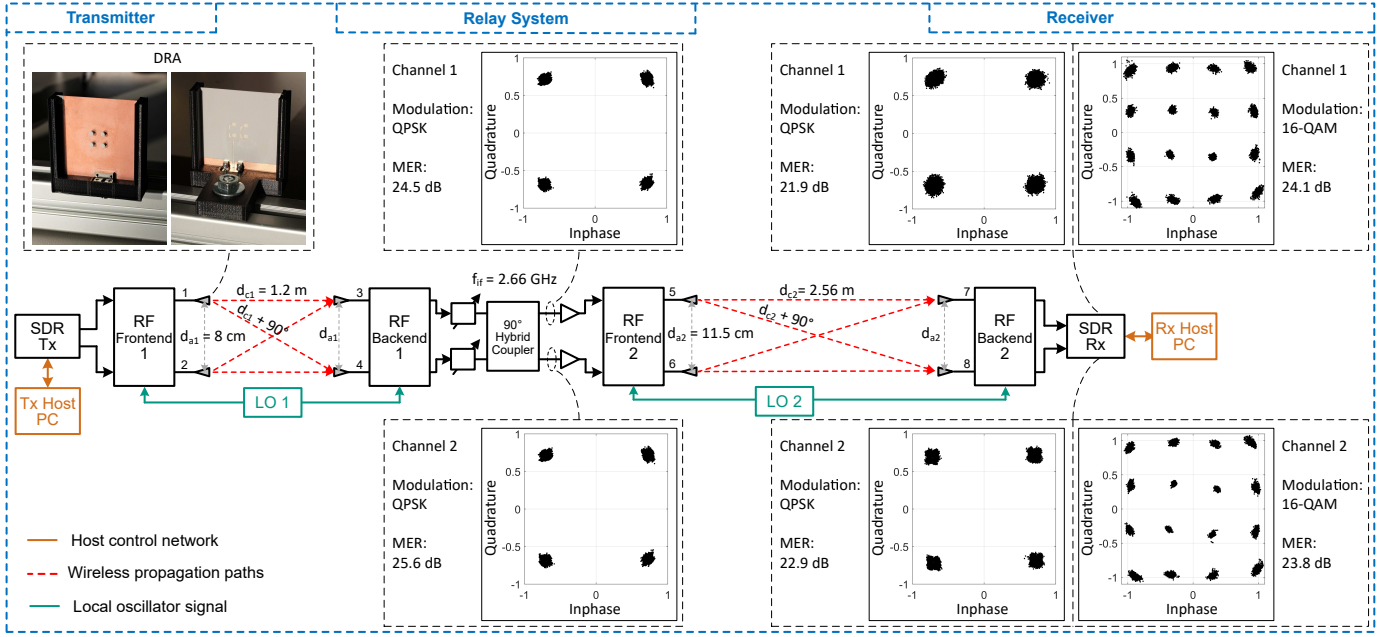


Fig. 1. Block diagram and results of the  $2 \times 2$  LoS MIMO relay system operating at 28 GHz.

between the receive chains can not be avoided and have to be calibrated out.

Considering a frequency non-selective  $2 \times 2$  LoS MIMO scenario with  $d_{\text{opt}}(i = 0)$  the MIMO channel matrix results to

$$\mathbf{H} = \begin{pmatrix} j & 1 \\ 1 & j \end{pmatrix} \quad (3)$$

and the output of the  $90^\circ$  hybrid coupler can be calculated as

$$\begin{aligned} \vec{z} &= \mathbf{T} \cdot \vec{y} \\ &= \frac{-1}{\sqrt{2}} \begin{pmatrix} j & 1 \\ 1 & j \end{pmatrix} \begin{pmatrix} 1 & j \\ j & 1 \end{pmatrix} \begin{pmatrix} x_1 \\ x_2 \end{pmatrix} + \mathbf{T} \cdot \vec{n} \\ &= \frac{-2j}{\sqrt{2}} \begin{pmatrix} x_1 \\ x_2 \end{pmatrix} + \mathbf{T} \cdot \vec{n} \end{aligned} \quad (4)$$

with the received signal vector  $\vec{y} = (y_1, y_2)^T$  represented by

$$\vec{y} = \mathbf{H} \vec{x} + \vec{n} \quad (5)$$

where  $\vec{x} = (x_1, x_2)^T$  represents the transmitted signal vector and  $\vec{n}$  denotes an additive random white Gaussian noise vector. It is shown by Eq. 4 that by using an ideal  $90^\circ$  hybrid coupler the influence of the LoS MIMO channel can be removed and the two in air combined data streams sent by the two transmit antennas can be separated at the receiver. However, in case of a non-ideal antenna spacing the coefficients of the MIMO channel matrix change, which results in a reduced decoupling between the two transmitted data streams and thereby a reduced reachable spectral efficiency. Furthermore, multipath propagation may decrease the spectral efficiency as time delayed replicas of the two transmit signals would interfere and cause inter-symbol-interferences (ISI). To avoid ISI the maximum excess delay has to be smaller than the symbol duration, i.e. the channel is considered as frequency-nonselective [25].

### B. Analysis of Non-ideal Relay Systems

Assuming a non-ideal  $2 \times 2$  LoS MIMO relay system the received signal at the last receiver results to

$$\begin{aligned} \vec{w} &= \mathbf{H}_2 \mathbf{T} \mathbf{H}_1 \vec{x} + \vec{n} \\ &= \begin{pmatrix} \epsilon_{11}^2 & j\epsilon_{12}^2 \\ j\epsilon_{21}^2 & \epsilon_{22}^2 \end{pmatrix} \frac{-1}{\sqrt{2}} \begin{pmatrix} jt_{11}^\epsilon & t_{12}^\epsilon \\ t_{21}^\epsilon & jt_{22}^\epsilon \end{pmatrix} \\ &\quad \cdot \begin{pmatrix} \epsilon_{11}^1 & j\epsilon_{12}^1 \\ j\epsilon_{21}^1 & \epsilon_{22}^1 \end{pmatrix} \begin{pmatrix} x_1 \\ x_2 \end{pmatrix} + \hat{\vec{n}} \end{aligned} \quad (6)$$

with the error channel coefficients  $\epsilon_{xx}^1$  and  $\epsilon_{xx}^2$  of the first and second MIMO channel matrices  $\mathbf{H}_1$  and  $\mathbf{H}_2$ , respectively. The errors introduced by a non-ideal equalization within the relay are denoted as  $t_{xx}^\epsilon$ . The influences of a non-ideal channel matrix, e.g. caused by a misalignment of the antennas, are investigated by the authors in [23]. Therefore, we only focus on errors introduced by the non-ideal relay system, i.e.  $\epsilon_{xx}^1 = \epsilon_{xx}^2 = 1$  and  $\mathbf{H}_1 = \mathbf{H}_2 = \mathbf{H}$ . For simplification only symmetric errors in amplitude and phase are considered for the relay system, i.e.  $t_d^\epsilon = t_{11}^\epsilon = t_{22}^\epsilon$  and  $t_c^\epsilon = t_{12}^\epsilon = t_{21}^\epsilon$ . This assumption is valid, as the employed  $90^\circ$  hybrid coupler is symmetric and operated at the intermediate frequency (IF) around 2.66 GHz, which reduces the influence of manufacturing errors. The considered amplitude and phase imbalances denoted by  $A_e$  and  $\varphi_e$  lead to the coefficients  $t_d^\epsilon = (1 + \frac{A_e}{2}) \cdot e^{j \cdot (\varphi_e/2)}$  and  $t_c^\epsilon = (1 - \frac{A_e}{2}) \cdot e^{j \cdot (-\varphi_e/2)}$ . As performance metric serves the spectral efficiency or maximum sum rate given in bps/Hz, which can be calculated by [26]

$$R = \log_2 \left\{ \left| \mathbf{I}_{N_{\text{ant}}} + \frac{\gamma}{M_{\text{ant}}} \hat{\mathbf{H}} \hat{\mathbf{H}}^H \right| \right\} \quad (7)$$

with the normalized channel matrix  $\|\hat{\mathbf{H}}\|^2 = N_{\text{ant}} M_{\text{ant}}$ , where  $M_{\text{ant}}$  and  $N_{\text{ant}}$  denote the number of transmit and receive antennas and  $\mathbf{I}_{N_{\text{ant}}}$  represents the identity matrix of dimension  $N_{\text{ant}}$ . To calculate the spectral efficiency of the overall relay

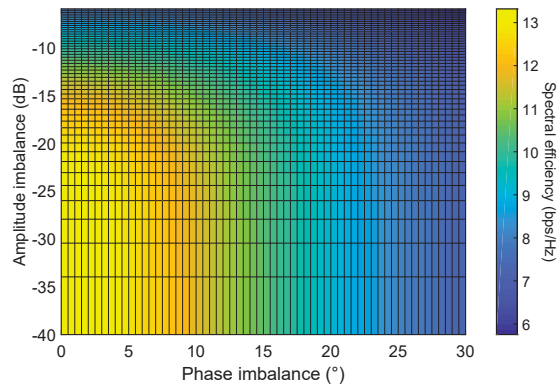


Fig. 2. Influences of amplitude and phase imbalances within the relay system onto the spectral efficiency of a  $2 \times 2$  LoS MIMO relay system.

connection the total channel matrix results to  $\hat{H} = H_2TH_1$  as shown in eq. 6. Furthermore, the signal-to-interference-plus-noise ratio (SINR)  $\gamma$  has to be considered, as a non-ideal equalization within the relay would lead to crosstalk between the two uncorrelated transmit data streams. The SINR introduced by a non-ideal equalization within the relay system results to

$$\gamma = \frac{P_s}{P_i + P_n} = \frac{|t_d^\epsilon + t_c^\epsilon|^2}{|t_d^\epsilon - t_c^\epsilon|^2 + P_n} \quad (8)$$

where  $P_n$  represents the noise power. Based on the presented equations the spectral efficiency is calculated considering imbalances in amplitude and phase of the relay system as shown in Fig. 2. The noise power is kept constant with a signal-to-noise ratio (SNR) of 20 dB. The results show that for small phase imbalances the loss in spectral efficiency is considerably low. A phase imbalance of  $\varphi_e = 5^\circ$  leads to a loss in spectral efficiency of 0.5 bps/Hz, considering a sufficiently low amplitude imbalance ( $< -40$  dB). To limit the loss in spectral efficiency to 0.5 bps/Hz the amplitude imbalances should be less than  $-21$  dB, in case the phase imbalances are negligible. These results give important feedback to the design requirements of the  $90^\circ$  hybrid coupler or more general the analog equalization network and help finding the optimal operation frequency.

### III. LOS MIMO RELAY SETUP

To verify the analog channel equalization using a  $90^\circ$  hybrid coupler a relay system operating at 28 GHz has been developed. To achieve a higher robustness against amplitude and phase imbalances, introduced for example by manufacturing tolerances, the  $90^\circ$  hybrid coupler operates at the IF of 2.66 GHz within a heterodyne system architecture. It should be noted, that the  $90^\circ$  hybrid coupler may be directly integrated within the RF front- and backend without requiring up- and down-conversion to IF. The block diagram of the relay system is shown in Fig. 1. At the first transmitter and last receiver end software defined radio (SDR) from Ettus Research Inc. of type USRP X310 are utilized, which perform analog-to-digital and digital-to-analog conversion as well as baseband to IF up- and down-conversion, amplification and filtering. The radio frequency (RF) front- and backends perform IF to RF

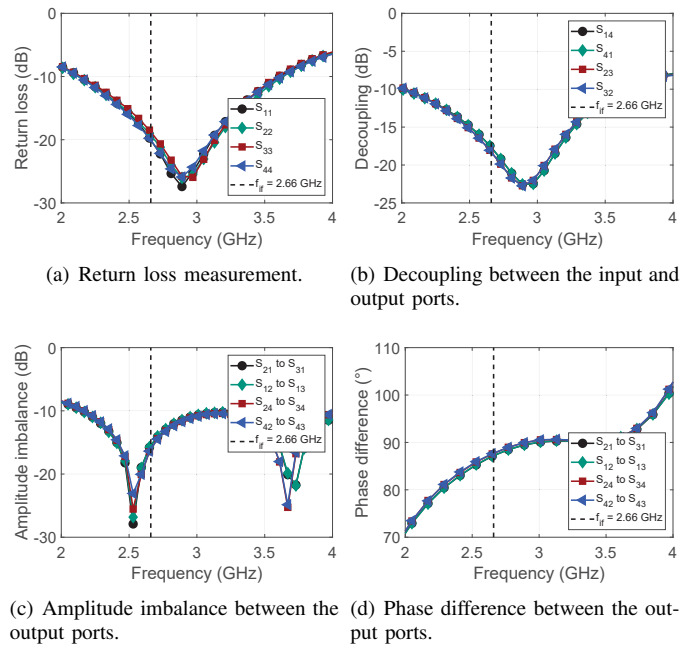


Fig. 3. Measurement results of the  $90^\circ$  hybrid coupler.

conversion as well as amplification and bandpass filtering as presented by the authors in [27]. To avoid frequency offsets between the transmitter and receiver, the local oscillators (LO) for the RF front- and backends and the SDRs are synchronized using a 10 MHz reference signal. As the receiver of the first  $2 \times 2$  LoS MIMO link introduces itself imbalances in amplitude and phase due to non-phase-matched cables, deviations within the RF chains, manufacturing tolerances of the housing and circuit boards, etc. these imbalances are calibrated out upfront using mechanical adjustable phase shifters and variable attenuators in front of the  $90^\circ$  hybrid coupler. The coupler itself is manufactured using standard two metal layer printed circuit board (PCB) and FR-4 as substrate with 0.6 mm thickness. The measurement results are depicted in Fig. 3. At the utilized IF of 2.66 GHz the return loss is better than 18 dB and the introduced transmission losses are around 1 dB. The phase difference at 2.66 GHz of the outputs differs from the ideal  $90^\circ$  by  $3.3^\circ$  and the amplitude imbalances are around  $-16$  dB. The measured isolation between the input ports is 17 dB. Using the results shown in Fig. 2 the loss in spectral efficiency introduced by the  $90^\circ$  hybrid coupler at 2.66 GHz is 1.5 bps/Hz. By selecting the IF to 2.55 GHz this loss could be reduced to 0.8 bps/Hz.

As antennas eight identical  $2 \times 2$  dielectric resonator antenna arrays are designed, measured and built up. The antennas use a standard two metal layer PCB process for the feeding structure and 3D printing for fabrication of the dielectric resonators. The PCB consists of a 203  $\mu$ m thick Rogers 4003 substrate. The cylindrical dielectric elements are printed using an Ultimaker 3 Extended 3D printer with the dielectric material Preperm L450 offering an  $\epsilon_r$  of 4.5. The feeding of the dielectric resonators is done via two elliptical monopole elements radiating into a circular slot within the ground plane. The monopoles are thereby fed with a  $180^\circ$  phase shift. The 3D printed dielectric

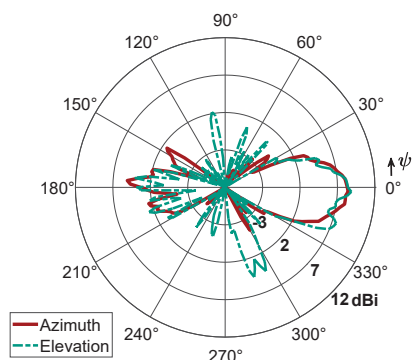


Fig. 4. Antenna pattern in azimuth and elevation of the  $2 \times 2$  dielectric resonator antenna array.

resonator elements are placed manually and glued onto the circular slots using Loctite 406 adhesive. The antennas are characterized by its large bandwidth covering the full 3 GHz of the  $n257$  band with an measured antenna array gain of larger than 7.6 dBi and a return loss of better than 10 dB. At the carrier frequency used within the measurements of 28 GHz each array achieves a gain of 8.7 dBi. The half-power beamwidth in azimuth is  $34^\circ$ . The antenna pattern of the antenna in azimuth and elevation is given in Fig. 4. A photo of the front and back of the antenna with its 3D printed holder is shown in Fig. 1. A dual-polarized version of the DRA with a more detailed description is presented by the authors in [28].

To avoid any multipath propagation the measurements took place in an anechoic chamber. The ideal antenna spacings are calculated using equation 1 and result for the first link with a distance of 1.2 m to an antenna spacing of 8 cm and for the second link with a distance of 2.56 m to an antenna spacing of 11.5 cm. A photo of the relay system is shown in Fig. 5.

#### IV. MEASUREMENT RESULTS

To analyse the performance of the relay system two uncorrelated data streams are generated at the first transmitter. As signal waveform QPSK and 16-QAM signals are utilized with a frame length of 2000 symbols. Furthermore, pulse-shaping of the transmit signals is performed using a Root-Raised-Cosine filter with roll-off factor of 0.35 and an oversampling factor of 16. The output sample rate of the SDR is set to 4 MHz. At the final receiver the data is recorded for several seconds and evaluated in post-processing.

At first the constellation diagrams and MERs at the output ports of the  $90^\circ$  hybrid coupler are determined. Therefore, a SDR is connected to the output of the  $90^\circ$  hybrid coupler enabling the digitalization of the output signals. In post-processing only downsampling using matched filtering is performed, meaning no digital equalization takes place. The results are shown within the block diagram in Fig. 1. For a QPSK signal a MER of higher than 24.5 dB could be achieved for both channels. To analyse the cross-coupling between the two channels only one transmitter is activated and the received power at both outputs of the  $90^\circ$  hybrid coupler is compared. Thereby a decoupling of the channels of more than 27 dB could be achieved. The separated signals after the  $90^\circ$  hybrid

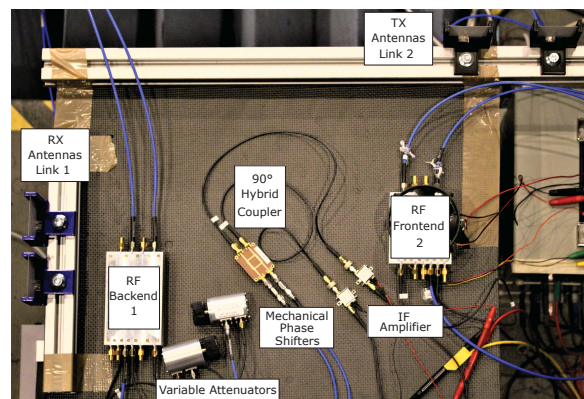


Fig. 5. Photo of the relay setup including the receive antennas of the first LoS MIMO link on the left side and the transmit antennas of the second LoS MIMO link on the top right of the photo. The antenna modules are mounted on rails to precisely adjust the spacing between them. The variable attenuators 50R-408 from *JFW Industries* have a total range of 10 dB and can be adjusted in 1 dB steps. The mechanical adjustable phase shifters LS-0170-1121 from *Spectrum Elektrotechnik GmbH* offer a nominal phase shift of  $0.36^\circ/\text{GHz}/\text{Turn}$ .

coupler are then up-converted and transmitted by the second  $2 \times 2$  LoS MIMO link. At the final receiver the signals are digitally equalized using an estimate of the MIMO channel matrix of the total link. The required estimation of the MIMO channel matrix for equalization is performed by separating the two transmit signals using code division multiple access (CDMA). It should be noted, that in real systems the separation by CDMA is only required during the channel estimation process, which has to be repeated according to the coherence time of the channel. The results are displayed in Fig. 1 as well. Compared to the results after the  $90^\circ$  hybrid coupler the MER slightly decreased by less than 3 dB to 21.9 dB for channel 1 and 22.9 dB for channel 2 respectively. Moreover, the signal quality at the last receiver is shown for a 16-QAM signal achieving a high MER of 24.1 dB and 23.8 dB for channel 1 and 2 respectively.

To put the results into perspective, the signal quality is compared to a SISO relay transmission by turning off one of the two virtual channels. This means, that either the antennas in Fig. 1 labeled 1,3,5,7 or the antennas labeled 2,4,6,8 are active. The achieved MER values at the final receiver end are with 21.9 dB for channel 1 and 24.0 dB for channel 2 similar to the ones for the  $2 \times 2$  LoS MIMO link. Consequently, the link performance is not limited by the interference between the two parallel links, but rather by the noise of the link itself.

#### V. CONCLUSION

This work presents a novel  $2 \times 2$  LoS MIMO relay system operating at 28 GHz using a simple  $90^\circ$  hybrid coupler for analog channel equalization. To the best of our knowledge this is the first realized and measured analog LoS MIMO relay system. The measurement results show a high decoupling of the channels of more than 27 dB and MER values of 22 dB at the total link end. The results prove the practical feasibility of the system concept realizing a low-cost and hardware efficient solution for relay systems connecting directional wireless communication links.

## REFERENCES

- [1] J. G. Andrews, S. Buzzi, W. Choi, S. V. Hanly, A. Lozano, A. C. K. Soong, and J. C. Zhang, "What Will 5G Be?" *IEEE Journal on Selected Areas in Communications*, vol. 32, no. 6, pp. 1065–1082, jun 2014.
- [2] H. Viswanathan and M. Weldon, "The Past, Present, and Future of Mobile Communications," *Bell Labs Technical Journal*, vol. 19, pp. 8–21, 2014.
- [3] T. S. Rappaport, S. Sun, R. Mayzus, H. Zhao, Y. Azar, K. Wang, G. N. Wong, J. K. Schulz, M. Samimi, and F. Gutierrez, "Millimeter wave mobile communications for 5G cellular: It will work!" *IEEE Access*, vol. 1, pp. 335–349, 2013.
- [4] *Technical Specification Group Radio Access Network; New frequency range for NR (24.25–29.5 GHz) (Release 15)*, 3rd Generation Partnership Project (3GPP), jun 2018, v1.0.0 (2018-06).
- [5] M. Jaber, M. A. Imran, R. Tafazolli, and A. Tukmanov, "5G Backhaul Challenges and Emerging Research Directions: A Survey," *IEEE Access*, vol. 4, pp. 1743–1766, 2016.
- [6] S. Rangan, T. S. Rappaport, and E. Erkip, "Millimeter-Wave Cellular Wireless Networks: Potentials and Challenges," *Proceedings of the IEEE*, vol. 102, no. 3, pp. 366–385, mar 2014.
- [7] L. Bao and B. E. Olsson, "Methods and measurements of channel phase difference in 2x2 microwave LOS-MIMO systems," *IEEE International Conference on Communications*, vol. 2015-September, pp. 1358–1363, 2015.
- [8] C. Sheldon, E. Torkildson, Munkyo Seo, C. Yue, U. Madhow, and M. Rodwell, "A 60GHz line-of-sight 2x2 MIMO link operating at 1.2Gbps," in *2008 IEEE Antennas and Propagation Society International Symposium*. IEEE, jul 2008, pp. 1–4.
- [9] M. Sjodin, P. Ligander, L. Bao, and J. Hansryd, "A 40.2 bps/Hz Single Polarization 4x4 Line-of-Sight MIMO Link With Unsynchronized Oscillators," in *2019 IEEE Radio and Wireless Symposium (RWS)*, vol. 1. IEEE, jan 2019, pp. 1–3.
- [10] D. Cvetkovski, E. Grass, T. Halsig, and B. Lankl, "Hardware-in-the-loop demonstration of a 60GHz line-of-sight 2x2 MIMO link," *17th IEEE International Conference on Smart Technologies, EUROCON 2017 - Conference Proceedings*, no. July, pp. 631–636, 2017.
- [11] T. Halsig, D. Cvetkovski, E. Grass, and B. Lankl, "Measurement Results for Millimeter Wave Pure LOS MIMO Channels," in *2017 IEEE Wireless Communications and Networking Conference (WCNC)*, no. 1. IEEE, mar 2017, pp. 1–6.
- [12] C. Zhou, X. Chen, X. Zhang, S. Zhou, M. Zhao, and J. Wang, "Antenna array design for los-mimo and gigabit ethernet switch-based Gbps radio system," *International Journal of Antennas and Propagation*, vol. 2012, 2012.
- [13] M. H. Castaneda Garcia, M. Iwanow, and R. A. Stirling-Gallacher, "LOS MIMO Design Based on Multiple Optimum Antenna Separations," *IEEE Vehicular Technology Conference*, vol. 2018-August, 2019.
- [14] Y. H. Cho and J. J. Kim, "Line-of-sight MIMO channel in millimeter-wave beamforming system: Modeling and prototype results," *IEEE Vehicular Technology Conference*, vol. 2015, no. 3, pp. 1–5, 2015.
- [15] P. Driessen and G. Foschini, "On the capacity formula for multiple input-multiple output wireless channels: a geometric interpretation," *IEEE Transactions on Communications*, vol. 47, no. 2, pp. 173–176, 1999.
- [16] F. Bohagen, P. Orten, and G. Oien, "Design of Optimal High-Rank Line-of-Sight MIMO Channels," *IEEE Transactions on Wireless Communications*, vol. 6, no. 4, pp. 1420–1425, apr 2007.
- [17] L. Leilei, H. Wei, W. Haiming, Y. Guangqi, Z. Nianzu, Z. Hongxin, C. Jing, Y. Cheng, Y. Xutao, T. Hongjun, Z. Hongbin, and T. Ling, "Characterization of line-of-sight MIMO channel for fixed wireless communications," *IEEE Antennas and Wireless Propagation Letters*, vol. 6, pp. 36–39, 2007.
- [18] C. Sheldon, E. Torkildson, M. Seo, C. P. Yue, M. Rodwell, and U. Madhow, "Spatial multiplexing over a line-of-sight millimeter-wave MIMO link: A two-channel hardware demonstration at 1.2Gbps over 41m range," *Proceedings of the 1st European Wireless Technology Conference, EuWiT 2008*, no. October, pp. 198–201, 2008.
- [19] Z. Li, L. Zhou, A. Honda, and Y. Ohashi, "Spatial multiplexing of 4x4 UCA LoS MIMO systems with splitting matrix at RF band," *2015 9th European Conference on Antennas and Propagation, EuCAP 2015*, no. 4, pp. 1–4, 2015.
- [20] B. S. Kim, M. S. Kang, K. S. Kim, W. J. Byun, M. S. Song, and H. C. Park, "18 GHz 2x2 analog LoS MIMO test-bed system with fully controlled ICM," *2016 International Conference on Information and Communication Technology Convergence, ICTC 2016*, pp. 1023–1025, 2016.
- [21] Y. Yan, P. Bondalapati, A. Tiwari, C. Xia, A. Cashion, D. Zhang, Q. Tang, and M. Reed, "11-Gbps Broadband Modem-Agnostic Line-of-Sight MIMO Over the Range of 13 km," *2018 IEEE Global Communications Conference, GLOBECOM 2018 - Proceedings*, pp. 1–7, 2018.
- [22] X. Song, T. Halsig, W. Rave, B. Lankl, and G. Fettweis, "Analog equalization and low resolution quantization in strong line-of-sight MIMO communication," *2016 IEEE International Conference on Communications, ICC 2016*, 2016.
- [23] Y. Li, J. Eisenbeis, R. Míchev, M. B. Alabd, and T. Zwick, "Measurement-based Misalignment Analysis of Dual-polarized 2 x 2 Line-of-Sight MIMO System at 28 GHz," 2020, manuscript submitted for publication.
- [24] D. M. Pozar, *Microwave Engineering, 4th Edition*. Wiley, 2011.
- [25] B. Sklar, "Rayleigh fading channels in mobile digital communication systems .II. Mitigation," *IEEE Communications Magazine*, vol. 35, no. 7, pp. 102–109, jul 1997. [Online]. Available: <http://ieeexplore.ieee.org/document/601748/>
- [26] S. Loyka and G. Levin, "On physically-based normalization of MIMO channel matrices," *IEEE Transactions on Wireless Communications*, vol. 8, no. 3, pp. 1107–1112, mar 2009. [Online]. Available: <http://ieeexplore.ieee.org/document/4801454/>
- [27] J. Eisenbeis, M. Tingulstad, N. Kern, Z. Kollár, J. Kowalewski, P. Ramos López, and T. Zwick, "MIMO Uplink Communication Measurements in Small Cell Scenarios at 28 GHz," 2020, manuscript submitted for publication.
- [28] J. Kowalewski, J. Eisenbeis, A. Jauch, J. Mayer, M. Kretschmann, and T. Zwick, "A Broadband Dual-Polarized Dielectric Resonator Antenna for Next Generation Mobile Radio," 2020, manuscript submitted for publication.